

pubs.acs.org/JACS Article

Ligand-Field Spectroscopy of Co(III) Complexes and the Development of a Spectrochemical Series for Low-Spin d⁶ Charge-**Transfer Chromophores**

Jonathan T. Yarranton and James K. McCusker*



Cite This: J. Am. Chem. Soc. 2022, 144, 12488-12500



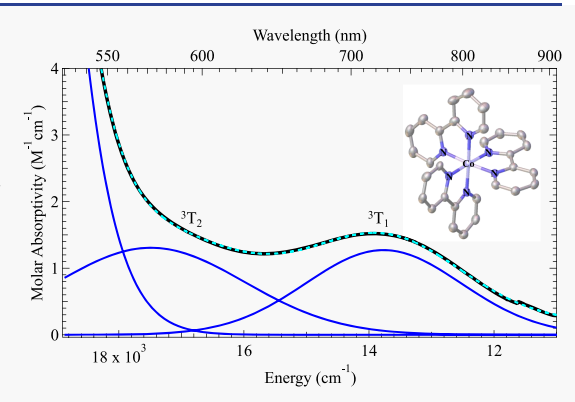
ACCESS I

Metrics & More

Article Recommendations

Supporting Information

ABSTRACT: A study of a series of six-coordinate Co(III) complexes has been carried out to quantify spectroscopic parameters for a range of ligands that are commonly employed to realize strong charge-transfer absorptions in low-spin, d⁶ systems. Identification of any three ligand-field transitions allows for the determination of the splitting parameter (10 Dq) as well as the Racah B and C parameters for a given compound. The data revealed a relatively small spread in the magnitude of 10 Dq, ranging from ca. 23 000 cm⁻¹ in the case of [Co(pyrro-bpy)₃]³⁺ (where pyrro-bpy is 4,4'-dipyrrolidinyl-2,2'bipyridine) to ca. 26 000 cm⁻¹ for $[Co(terpy)_2]^{3+}$ (where terpy is 2,2':6',2"terpyridine). Significantly, trends across the series suggest that polypyridyl ligands behave as net π -donors when interacting with Co(III), in contrast to the net π -accepting character they exhibit when bound to second- and thirdrow metals. The influence of strong σ donation associated with carbene-



based ligands was evident from the data acquired for [Co(BMeImPy)₂]³⁺ (where BMeImPy is 3,3'-(pyridine-2,6-diyl)bis(1-methyl-1H-3-imidazolium)), where a 10 Dq value of ca. 30 000 cm⁻¹ was determined. Spectroscopic data were also analyzed for [Fe(bpy)₃]²⁺ using the results on [Co(bpy)₃]³⁺ as a reference point. A value for 10 Dq of 21 000 cm⁻¹ was estimated, indicating a reduction in the ligand-field strength of ca. 3000 cm⁻¹ upon replacing Co(III) with Fe(II). We suggest that this approach of taking advantage of the blueshift of the charge-transfer feature in Co(III) complexes to reveal otherwise obscured ligand-field bands can be a useful tool for the development of new ligand systems to expand the photofunctionality of first-row transition-metal-based chromophores.

INTRODUCTION

The photophysical properties of first-row metal complexes have experienced renewed interest over the past several years due to the emergent recognition of the value of earth-abundant alternatives to the more commonly employed second- and third-row transition-metal-based chromophores for a variety of photolytic applications. 1-3 Many of these applications focus on electron transfer processes, where the absorbed light results in the formation of an excited state that can facilitate the oxidation or reduction of substrates ranging from semiconductors in the case of photovoltaics (e.g., dye-sensitized solar cells)^{4,5} to organic molecules in the rapidly expanding field of photoredox catalysis.⁶ Although there are circumstances in which ligand-field excited states can engage in electron transfer chemistry, 7-9 charge-transfer excited states are more predisposed toward this type of chemistry due to the fact that light absorption directly results in the creation of chemical potential in the form of a charge-separated species. While the absorptive properties of many first-row metal complexes are dominated by intense charge-transfer bands in much the same way as their second- and third-row congeners, the relative energies of their charge-transfer and ligand-fieldstate manifolds are such that ultrafast conversion from the former to the latter outpaces the desired charge-transfer-based chemistry. The origin of this situation can be linked to the primogenic effect, 10 resulting in weaker metal-ligand interactions in the first-transition series relative to other regions of the transition block and impacts a host of physical and photophysical properties, including the propensity toward photoinduced electron transfer.

Identification of the nature of this problem has spurred considerable research activity into finding ways around this situation to create new classes of first-row chromophores whose photophysical properties resemble compounds like [Ru(bpy)₃]²⁺ and Ir(ppy)₃. The most successful approaches have exploited the strong σ -donating characteristics of carbene and isocyanide ligands. The pioneering example was published

Received: May 9, 2022 Published: June 24, 2022





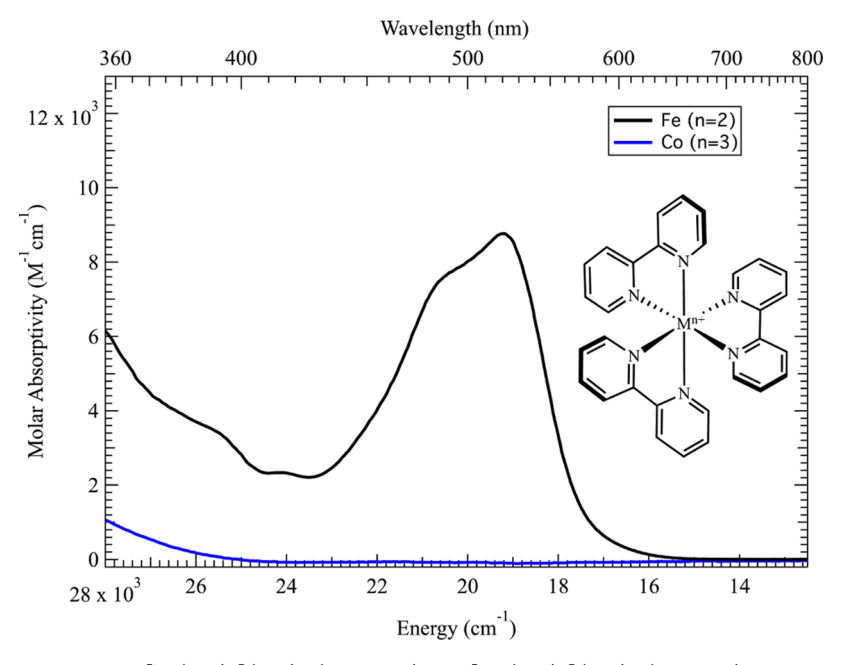


Figure 1. Electronic absorption spectra of $[Fe(bpy)_3](PF_6)_2$ (black line) and $[Co(bpy)_3](PF_6)_3$ (blue line) in CH₃CN solution. The plots reveal the significant difference in the optical characteristics of these isoelectronic species due to the change in character of the charge-transfer band from MLCT in the case of Fe(II) to LMCT in the case of Co(III).

by Wärnmark and co-workers in 2013,¹¹ but this has since been followed by and expanded upon through work from a number of groups including Wenger,¹² Heinze,¹³ Bauer,^{14,15} Herbert,^{16,17} and Gros^{18,19} to name a few. A less well-developed but potentially promising approach of exploiting information from quantum coherence was recently demonstrated by us,²⁰ but for both of these research threads, the problem ultimately distills down to synthetic design. Proper synthetic design in turn relies on an understanding of the key parameters that are needed to create an electronic structure in a first-row metal complex that mimics what is easily realized in the second- and third-transition series.

The success achieved with ligand motifs such as Nheterocyclic carbenes derives from the strong ligand field that these sorts of molecules present to the metal ion. The energetics of charge-transfer states are more closely aligned with redox potentials (e.g., the oxidation potential of the metal and reduction potential of the ligand for metal-to-ligand charge-transfer states), so approaches that target ligand-field strength rely on destabilizing the ligand-field excited states such that the CT state(s) are the lowest-energy excited states of the system. Recent work from our group suggests that these two factors can be independently controlled, 21 but a significant challenge for realizing this energetic inversion stems from an inability to know in advance the ligand-field strength required to achieve the desired result. The problem stems from the fact that experimentally assessing ligand-field strengths is difficult if not impossible in most first-row systems of interest. For example, the electronic absorption spectrum of [Fe(bpy)₃]²⁺ shown in Figure 1 is dominated in the mid-visible by an intense feature assigned as a ${}^{1}A_{1} \rightarrow {}^{1}MLCT$ transition(s). The molar absorptivity of this band is on the order of 10 000 M⁻¹ cm⁻¹—exactly what one wants from the perspective of light capture—but its large oscillator strength simultaneously prevents an evaluation of the ligand-field strength associated with 2,2'-bipyridine because the (much weaker) d-d transitions that inform on ligand-field strength are buried

under the MLCT envelope. This is a conundrum that one is faced with across the first-transition series, i.e., ligands that facilitate the realization of intense absorption cross sections for light harvesting are at the same time obscuring certain features necessary to assess their ability to leverage that stored chemical potential.

The question of how to gauge ligand-field strength with an eye toward application-driven synthetic design is not new. Indeed, this issue was studied extensively in the area of spin-crossover chemistry, where the goal was to design systems whose ligand-field strength was comparable to the spin-pairing energy such that variations in temperature could drive interconversion between the low-spin and high-spin forms of a given compound. ^{22,23} A successful approach along these lines in the case of Fe(II) spin-crossover systems was to examine isoelectronic Co(III) analogs. ²⁴ The change in character of the charge-transfer band from MLCT in the case of Fe(II) to LMCT for Co(III) contributes to a dramatic blueshift of this absorption feature into the near-ultraviolet (Figure 1, blue line), thereby allowing the lower-intensity d—d bands in the visible region of the spectrum to be revealed.

In this report, we have used this same approach to create a strategy for developing what amounts to a spectrochemical series for charge-transfer complexes of six-coordinate d⁶ first-row metal complexes. Specifically, the synthesis and spectroscopic characterization of a range of Co(III) complexes has allowed us to quantify the field strengths that define these ligand systems; the observation of spin-forbidden bands has furthermore provided the necessary information to specify values not just for 10 Dq—the ligand-field-splitting parameter—but also independent values for other terms relevant to excited-state electronic structure. To our knowledge, these results provide the first experimental insights into the relative ligand-field strengths of commonly used ligands that effect light absorption by transition-metal-based charge-transfer states and, we believe, will contribute toward the realization of a roadmap

for the synthetic design of photofunctional chromophores based on first-row transition-metal ions.

EXPERIMENTAL SECTION

General. All reaction and spectroscopic solvents were obtained from Sigma-Aldrich Chemical Co. and used without further purification unless otherwise stated. Dry THF, MeCN, and DCM were obtained from a Solvtek solvent drying system. 2,2'-bipyridine (bpy), 4,4'-dimethyl-2,2'-bipyridine (4,4'-dmb), 5,5'-dimethyl-2,2'bipyridine (5,5'-dmb), and 4,4'-di(tert-butyl)-2,2'-bipyridine (dtb), 4,4'-dimethoxy-2,2'-bipyridine (OMe-bpy) were obtained from Oakwood Chemicals. 2,2':6',2"-terpyridine (terpy) and elemental bromine were obtained from Sigma-Aldrich. Co(ClO₄)₂·6H₂O and anhydrous CoBr2 were obtained from Alfa Aesar. CoCl2·6H2O was obtained from Spectrum Chemical. NOPF₆ was obtained from Acros Organics. NMR spectra were collected in the Max T. Rogers NMR Facility of Michigan State University on an Agilent 500 MHz spectrometer; spectra were referenced internally to the residual solvent peak. Elemental analyses were performed by Midwest Micro Labs. 4,4'-diethylester-2,2'-bipyridine (deeb),^{25,26} 4,4'-dichloro-2,2'bipyridine (Cl-bpy),²⁷ 3,3'-(pyridine-2,6-diyl)bis(1-methyl-1*H*-3-imi-Dipyriciane (CI-DPy), 3,3 -(pyridine-2,0-diyl)bis(1-methyl-1H-3-imidazolium) hexafluorophosphate ([B^{Me}ImPy](PF₆)₂), ²⁸ [Co(NH₃)₆]-Cl₃, ²⁹ [Co(en)₃]Cl₃, ³⁰ [Co(bpy)₃](PF₆)₃, ³¹ [Co(4,4'-dmb)₃]-(PF₆)₃, ³² [Co(5,5'-dmb)₃](PF₆)₃, ³² [Co(phen)₃](PF₆)₃, ³¹ [Co(dtb)₃](PF₆)₃, ³¹ [Co(eterpy)₂](PF₆)₃, ³³ [Co(Cl-bpy)₃](PF₆)₃, ³⁴ and [Co(CM₆ hrv)](PR) $\frac{35}{2}$ [Co(M₆ hrv)](PR) $\frac{$ [Co(OMe-bpy)₃](PF₆)₃³⁵ were all prepared by literature methods.

Synthesis of Tris-(4,4'-diethylester-2,2'-bipyiridine)cobalt-(II) hexafluorophosphate, [Co(deeb)₃](ClO₄)₂. An amount of 0.400 g of deeb (1.3 mmol, 3.3 equiv) was dissolved in 30 mL of CHCl₃. A solution of 0.147 g of Co(ClO₄)₂·6H₂O (0.40 mmol, 1.0 equiv) in 15 mL of acetone was added dropwise producing an orange solution. The solution was stirred overnight at room temperature; during the course of the reaction, a precipitate formed. The reaction mixture was filtered and washed with CHCl₃ and diethyl ether. The yellow solid was dried under vacuum. The complex was used without further purification. Yield: 0.329 g (72%).

Synthesis of Tris-(4,4'-diethylester-2,2'-bipyiridine)cobalt-(III) hexafluorophosphate, [Co(deeb)₃](PF₆)₃. An amount of $0.300 \text{ g of } [Co(deeb)_3](ClO_4)_2 (0.26 \text{ mmol}, 1.0 \text{ equiv}) \text{ was dissolved}$ in 20 mL of dry CH₂Cl₂ and 53 mg of solid NOPF₆ (0.31 mmol, 1.2 equiv) was added. The reaction stirred vigorously under N₂ for 2 h. The dark solution slowly became cloudy with a yellow precipitate. The DCM solvent was evaporated, and the complex was dissolved in minimal MeCN and excess $\mathrm{NH_4PF_6}$ was added and stirred for 30 min. Diethyl ether was added to crash out a pale yellow solid. It was filtered and washed with H2O, EtOH, and diethyl ether and dried under vacuum. It was recrystallized by slow diffusion of diethyl ether into an acetonitrile/ethanol solution. Yield: 0.253 g (70%). Anal. Calcd. (Found) for C₄₈H₄₈CoF₁₈N₆O₁₂P₃: C, 41.43 (40.98); H, 3.47 (3.52); N 6.03 (5.76). ¹H NMR (500 MHz, acetone- d_6): δ 9.66 (d, J = 1.9Hz, 2H), 8.25 (dd, J = 6.1, 1.9 Hz, 2H), 8.16 (d, J = 6.0 Hz, 2H), 4.48 (q, J = 7.2 Hz, 4H), 1.36 (t, J = 6.9 Hz, 6H).

Synthesis of Tris(4,4'-dipyrrolidinyl-2,2'-bipyridine)cobalt-(III) hexafluorophosphate, [Co(pyrro-bpy)₃](PF₆)₃. Starting from [Co(Cl-bpy)₃](PF₆)₃, 0.266 g (0.230 mmol, 1.00 equiv) was suspended in 30 mL of dry still methanol and 300 μ L of pyrrolidine (3.6 mmol, 16 equiv) was added. The solution instantly changed colors from yellow to red-orange, and the solution was heated overnight under N2. Once at reflux, 1-2 mL of MeCN was added to aid solubilization. The solution was cooled to room temperature and 0.371 g of NH₄PF₆ (2.30 mmol, 10.0 equiv) were added and stirred for 30 min. The solvent was removed, and the residue was suspended in 50 mL of water and vacuum-filtered. The orange solid was washed with H_2O (6 × 30 mL) and diethyl ether until a powder formed. The solid was dried under vacuum. It was recrystallized by slow diffusion of diethyl ether into an acetone/methanol solution. Yield: 0.221 g (70%). Anal. Calcd. (Found) for C₅₄H₆₆CoF₁₈N₁₂P₃: C, 47.10 (47.15); H, 4.83 (4.61); N 12.21 (11.81). ¹H NMR (500 MHz, acetone- d_6): δ 7.8 (d, J = 2.8 Hz, 2H), 6.98 (d, J = 7.1 Hz, 2H), 6.80 (dd, J = 7.2, 2.8 Hz, 2H), 3.62 (m, 4H), 3.47 (m, 4H), 2.09 (m, 8H).

Synthesis of Bis(2,6-di(3-methylimidazol-1-ylidene)pyridine)cobalt(III) hexafluorophosphate, [Co(B^{Me}ImPy)₂]-(PF₆)₃. The complex was synthesized using a modified literature procedure. To a suspension of 2.00 g of [B^{Me}ImPy](PF₆)₂ (3.76) mmol, 2.00 equiv) in 100 mL of dry THF, 1.322 g of LiHMDS (7.90 mmol, 4.20 equiv) in 20 mL of dry THF was added dropwise at -78 °C under nitrogen. The suspension stirred for 1 h at this temperature, affording a clear red-orange solution. A solution of 0.411 g of anhydrous CoBr₂ (1.88 mmol, 1.00 equiv) in 40 mL of dry THF was added dropwise over 10 min at -78 $^{\circ}$ C and stirred for an additional 2 h at this temperature. The reaction warmed to room temperature overnight affording a dark green solution. The dark solution was saturated in air for 45 min to effect the oxidization of Co(II) to Co(III), affording a light brown suspension. The solvent was removed in vacuo, and the crude was dissolved in acetone and the solution was filtered to remove any insoluble material. The filtrate was concentrated slightly and a saturated solution of $\ensuremath{\mathsf{KPF}}_{6(aq)}$ was added to precipitate the complex. The solid was filtered and washed with water and diethyl ether. The crude was recrystallized twice by slow diffusion of diethyl ether into acetonitrile, columned twice on Sephadex LH-20 with 70% acetone/H2O, and recrystallized again by slow diffusion of diethyl ether into an acetonitrile solution. Yield: 0.652 g (37%). Anal. Calcd. (Found) for C₂₆H₂₆CoF₁₈N₁₀P₃: C, 32.12 (32.01); H, 2.69 (2.83); N, 14.40 (14.14). ¹H NMR (500 MHz, acetone- d_6): δ 8.61 (t, J = 8.3 Hz, 2H), 8.61 (d, J = 2.1 Hz, 4H), 8.47 (d, J = 8.3 Hz, 4H), 7.58 (d, J = 2.1 Hz, 4H), 3.09 (s, 12H).

Electronic Absorption Spectroscopy. All electronic absorption spectra were acquired on a double-beam PerkinElmer Lambda 1050 spectrophotometer. Spin-allowed transitions were measured in matched 1 cm pathlength quartz cells at a concentration of ~6 mM, whereas spin-forbidden transitions were measured in a 10 cm pathlength quartz cell at concentrations of ~20 mM; for the latter, the divergence of the light beam through the longer-pathlength cell necessitated a manual subtraction of the solvent blank. Spectra for hexafluorophosphate salts were measured in spectroscopic-grade CH₃CN, whereas the chloride salts of $[Co(en)_3]^{3+}$ and $[Co(NH_3)_6]^{3+}$ were measured in spectroscopic-grade H₂O. Gaussian deconvolution was performed on each spectrum using IgorPro to accurately determine transition energies and molar absorptivities.

X-ray Crystallography. Crystals of appropriate size were selected and mounted on a nylon loop with paratone oil on an XtaLAB Synergy, Dualflex, HyPix diffractometer. The crystals were kept at a steady T = 100.0(2) K during data collection. The structures were solved with the ShelXT³⁶ solution program using intrinsic phasing and using Olex2 1.3³⁷ as the graphical interface. The model was refined with ShelXL 2018/3³⁸ using full-matrix least-squares minimization on F^2 .

One crystal, [Co(deeb)₃](PF₆)₃, was collected using a Bruker CCD (charge-coupled device)-based diffractometer equipped with an Oxford Cryostream low-temperature apparatus operating at 173 K. The total number of images was based on results from the program COSMO,³⁹ where redundancy was expected to be 4.0 and completeness of 100% out to 0.83 Å. Cell parameters were retrieved using APEX II⁴⁰ software and refined using SAINT on all observed reflections. Data reduction was performed using the SAINT software, ⁴¹ which corrects for Lp. Scaling and absorption corrections were applied using SADABS⁴² multiscan technique, supplied by George Sheldrick. The solution and refinement were carried out using the same programs as the previous crystals. Refinement statistics and structures can be found in the Supporting Information.

■ RESULTS AND DISCUSSION

The goal of this study was an evaluation of the field strength of ligands that are commonly employed to create charge-transfer absorption features in first-row, d⁶ metal complexes. The challenge lies in the combined influence of the relative intensities of charge-transfer vs ligand-field transitions and their spectral overlap, obfuscating any meaningful experimental assessment of ligand-field strength in this class of chromo-

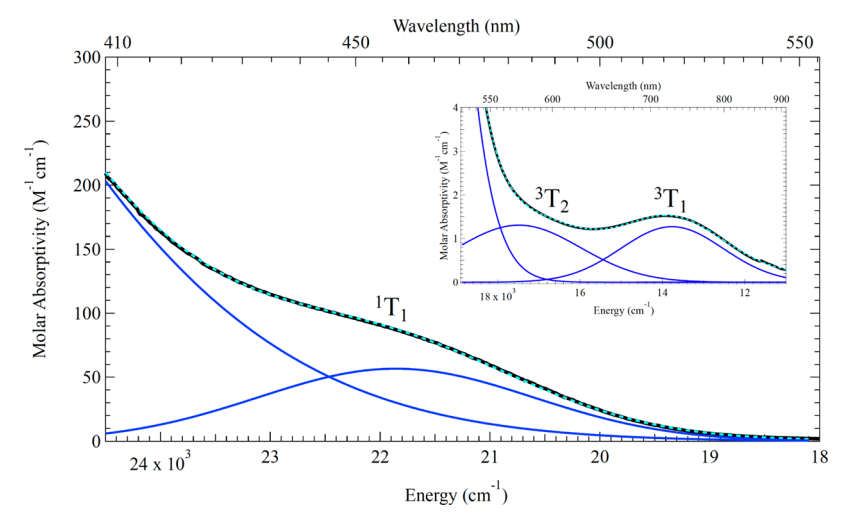


Figure 2. Electronic absorption spectrum of $[Co(bpy)_3](PF_6)_3$ in CH₃CN solution, highlighting the ligand-field transitions in the visible region. The blue solid lines show the result of Gaussian deconvolution of the spectrum using the minimum number of components required to fit the experimental spectrum. In the inset is plotted the spectrum obtained at $\lambda > 550$ nm obtained at a higher solute concentration in a 10 cm pathlength cell. The measured molar absorptivities of ca. 1 M⁻¹ cm⁻¹ indicates that these transitions are spin-forbidden.

phores. As indicated above, our approach takes inspiration from work in the 1970s and 1980s on spin-crossover complexes, in which isoelectronic Co(III) complexes were used as surrogates for the Fe(II) compounds of interest.²⁴ Although the visible spectra of most Fe(II) complexes containing aromatic ligands are dominated by metal-to-ligand charge-transfer (MLCT) transitions, the ligand-to-metal charge-transfer (LMCT) nature of transitions for Co(III) coupled with the increased potentials associated with reduction of Co(III) and oxidation of the aromatic ligands results in a substantial shift of the LMCT feature(s) to higher energy; in most cases, these bands now appear in the near-ultraviolet. This essentially opens up the visible region of the spectrum to where the much lower-intensity ligand-field absorptions are now readily observable. This is illustrated in Figure 2, which shows the ground-state absorption spectrum of $[Co(bpy)_3]^{3+}$ acquired in CH3CN solution. The red edge of the LMCT band, whose maximum is at 319 nm in the ultraviolet, can be seen tailing into the blue region of the spectrum. A pronounced shoulder evident on the low-energy portion of this band is easily resolved upon Gaussian deconvolution of the spectrum as a broad feature centered near 460 nm; its molar absorptivity of ~60 M⁻¹ cm⁻¹ is consistent with an assignment as a spin-allowed, Laporte-forbidden d-d band.

Substantially increasing the concentration of the solution and employing 10 cm pathlength optical cells allowed us to further observe one extremely weak but cleanly resolved absorption feature red of 700 nm, as well as a small inflection at higher energy that appears as a shoulder on the low-energy tail of the spin-allowed d–d band (Figure 2, inset). Gaussian deconvolution revealed two broad absorption bands centered at 720 and 575 nm, each with molar absorptivities of $\sim\!1~{\rm M}^{-1}$ cm $^{-1}$ suggesting spin-forbidden origins for both transitions. The intensities and relative proximities of these three features thus allow for straightforward assignments of $^1{\rm A}_1 \rightarrow ^3{\rm T}_1$, $^1{\rm A}_1 \rightarrow ^3{\rm T}_2$, and $^1{\rm A}_1 \rightarrow ^1{\rm T}_1$ for the bands at 730, 575, and 460 nm, respectively.

With these assignments, it now becomes possible to determine values for 10 Dq and the Racah *B* and *C* parameters, which will serve to define the energetics of the entire excited ligand-field-state manifold of the compound. As a reminder,

these three parameters have their origins in formalisms first developed by Bethe⁴³ and expanded upon by many researchers over the years but most significantly by Condon and Shortley, 44 Racah, 45 Jørgensen, 46 Ballhausen, 47 Griffith, 48 and, of course, Tanabe and Sugano. 49,50 A perturbative treatment of electronic structure in the transition block can start from either an infinitely strong field, in which interelectronic repulsions are neglected and a hydrogen-like, one-electron picture can be invoked, or an infinitely weak field in which the dominant influence of electron-electron repulsion leads to a breakdown of the one-electron picture and the need to employ multielectronic terms states for describing the electronic structure. Most molecules lie somewhere between these two extremes, but the more ionic nature of bonding in the first-transition series (relative to the second- and third-row) places these systems closer to the freeion limit even in cases where the strength of the ligand field is sufficient to yield a low-spin ground state. Accordingly, the primary consideration of electron-electron repulsion and the use of multielectronic term states is the lens through which the electronic structures of such compounds-including the Co(III) complexes we are considering herein—must be viewed.

Following the excellent discussion of this topic by Schmidtke, 51 parameterization of the electron–electron repulsion terms breaks the problem up into a series of integrals that are grouped together according to the approach outlined by Condon and Shortley. 44 In the limit of spherical symmetry (i.e., free ion), the analysis reduces to a set of integrals describing the radial part of the orbital wavefunction $(R_{\rm a}(r))$ having the general form

$$F^{k} = \int_{0}^{\infty} \left[\int_{0}^{r_{2}} R_{a}^{2}(r_{1}) \frac{r_{1}^{k}}{r_{2}^{k+1}} r_{1}^{2} dr_{1} + \int_{r_{2}}^{\infty} R_{a}^{2}(r_{1}) \frac{r_{2}^{k}}{r_{2}^{k+1}} r_{1}^{2} dr_{1} \right] R_{a}^{2}(r_{2}) r_{2}^{2} dr$$

$$(1)$$

where symmetry restrictions limit the nonvanishing terms to even values of k (i.e., 0, 2, 4, etc.); the magnitudes of the integrals decrease with increasing k (so, $F^0 > F^2 > F^4$, etc.) with

only the first three terms being relevant for a d orbital-based configuration. For numerical convenience, new terms F^k are usually introduced wherein

$$F_2 = \frac{1}{49}F^2 \tag{2a}$$

and

$$F_4 = \frac{1}{441}F^4 \tag{2b}$$

A more widely familiar (and arguably more useful) formalism was introduced by Racah who defined three terms based on the Condon–Shortley parameters as shown in eqs 3

$$A = F_0 - 49F_4 \tag{3a}$$

$$B = F_2 - 5F_4 (3b)$$

$$C = 35F_4 \tag{3c}$$

Since electron—electron repulsion integrals must be positive in terms of their sign (i.e., electron—electron repulsions are destabilizing interactions), it follows from eqs 2 and 3 that

$$F_0 > 49F_4 \tag{4a}$$

$$F_2 > 5F_4 \tag{4b}$$

and, in general

$$C > B$$
 (4c)

The A term is common to all term state energy expressions of a given configuration and therefore cancels when assessing energy differences between states (e.g., a spectroscopic transition): given this, the utility of the Racah parameters lies in the fact that transitions between states corresponding to the highest value of S for a given configuration will only be a function of B, which greatly simplifies the analysis of absorption spectra in the weak-field limit.

Integrals of the form in eq 1 are rarely solved in practice, rather, the formalisms represented by eqs 2 and 3 are used to empirically fit experimentally measured absorption spectra. There are two approaches that can be pursued: (1) full-matrix diagonalization of the determinant representing the multi-electronic term states of, in the case of Co(III), the d⁶ configuration using an operator of the appropriate field symmetry (e.g., O_h), or (2) approximating this determinant using only the diagonal terms. The latter amounts to assuming an infinitely strong ligand field with a solution that corresponds to solving a series of linearly independent equations based on the expressions derived by Tanabe and Sugano; ^{49,50} for the four transitions of a d⁶ ion in O symmetry we will be considering herein, these are

$$\Delta E(^{1}T_{2} - {}^{1}A_{1}) = 10Dq + 16B - C$$
 (5a)

$$\Delta E(^{1}T_{1} - {}^{1}A_{1}) = 10Dq - C$$
 (5b)

$$\Delta E(^{3}T_{2} - {}^{1}A_{1}) = 10Dq + 8B - 3C$$
 (5c)

$$\Delta E(^{3}T_{1} - {}^{1}A_{1}) = 10Dq - 3C$$
 (5d)

Following this second, more commonly employed approach, the assignments of the bands for $[Co(bpy)_3]^{3+}$ corresponding to eqs 5b-5d affords values of 25 900, 470, and 4050 cm⁻¹ for 10 Dq, *B*, and *C*, respectively. Full-matrix diagonalization, which allows for mixing among the various term states, is most

conveniently done using Bendix's program, LIGFIELD.⁵² The corresponding values obtained for $[Co(bpy)_3]^{3+}$ using this approach are 24 480, 560, and 3900 cm⁻¹. The similarity between the two results indicates that the degree of off-diagonal mixing involving the three lowest-energy excited states of $[Co(bpy)_3]^{3+}$ is relatively low. A Tanabe–Sugano diagram specific for $[Co(bpy)_3]^{3+}$ based on our spectroscopic data and full-matrix diagonalization analysis is shown in Figure 3.

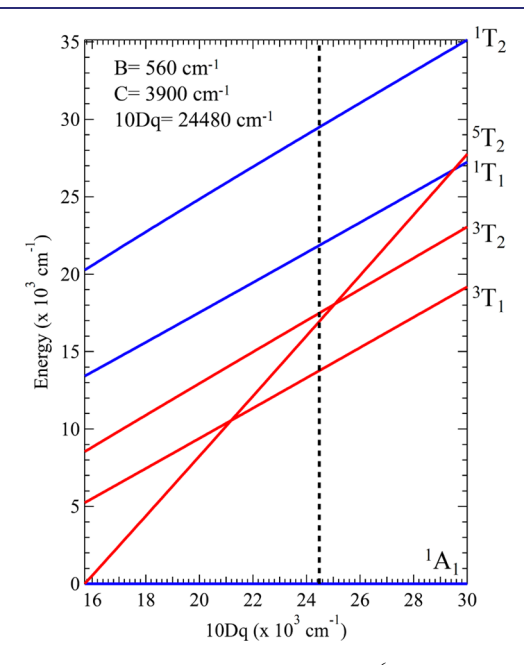
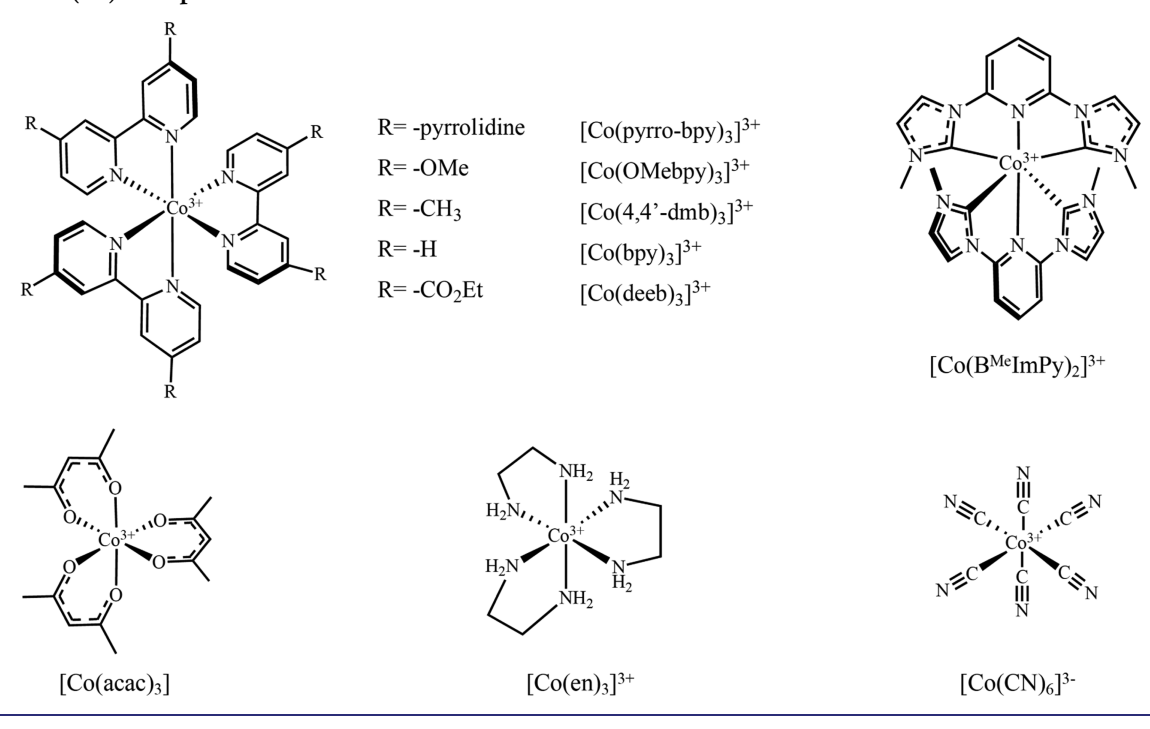


Figure 3. Tanabe—Sugano diagram for a d^6 O symmetry metal complex. The black dashed line corresponds to the position for $[Co(bpy)_3]^{3+}$ based on the experimentally determined values of 10 Dq, Racah B, and Racah C parameters shown in the inset.

A more detailed understanding of what these parameters tell us concerning the ligand-field strength of 2,2'-bipyridine—and more importantly what factors are critical in terms of ligand design for modulating the ligand-field strength—can be achieved by examining a series of compounds in which systematic changes in the composition of the ligand are correlated with changes in the ligand-field strength as gauged from their optical properties. We therefore undertook the synthesis of a series of Co(III) complexes consisting of (a) polypyridyl ligands with various substituents at the para and meta positions of the pyridine rings, representing different types of perturbations (e.g., σ -donating, π -accepting, etc.), (b) a carbene-based ligand, reflecting current trends in research on Fe(II)-based chromophores through the use of strongly σ donating ligands, and (c) several "classic" Co(III) coordination complexes (e.g., [Co(NH₃)₆]³⁺) to provide a baseline for comparisons across the series (Scheme 1).

Syntheses and Structures of $[Co(deeb)_3](PF_6)_3$, $[Co(pyrro-bpy)_3](PF_6)_3$, and $[Co(B^{Me}ImPy)_2](PF_6)_3$. Many of the compounds we prepared for this expanded assessment of the optical properties of Co(III) complexes are well known in the literature, but three of the compounds are new. In the case of $[Co(deeb)_3](PF_6)_3$, literature methods were used for the preparation of the ethyl ester ligand, which was then coordinated to cobalt(II) in a mixed solvent system of $CHCl_3$ and acetone; due to the lability of cobalt(II) and the

Scheme 1. Drawings of Several of the Compounds Prepared for the Creation of a Spectrochemical Series for Low-Spin, Six-Coordinate Co(III) Complexes



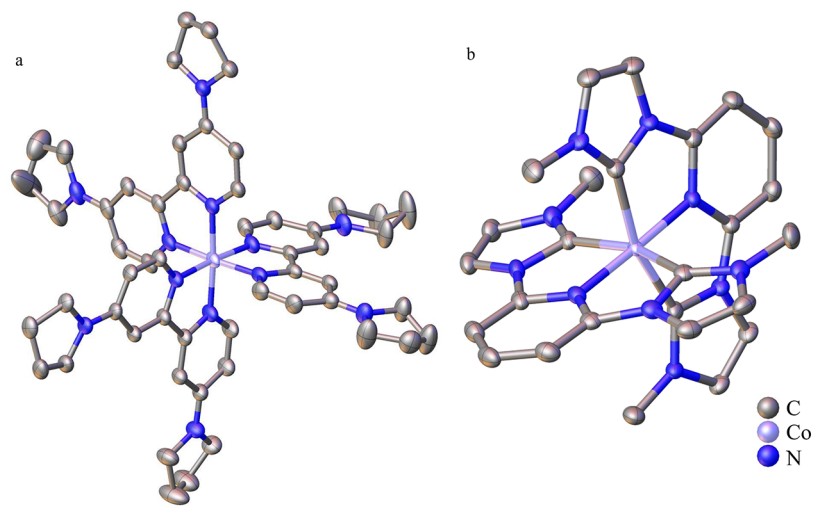


Figure 4. Single-crystal X-ray structures of the cations of (a) $[Co(pyrro-bpy)_3](PF_6)_3$ and (b) $[Co(B^{Me}ImPy)_2](PF_6)_3$. The metal ion is indicated in purple, nitrogen atoms in blue, and carbon atoms in gray; hydrogen atoms have been omitted for clarity. Details concerning structure refinement, bond distances, and angles can be found in the Supporting Information.

weaker coordination of electron-deficient bipyridyl ligands, this solvent system was chosen to minimize the formation of stable solvento species. Under these conditions, $[Co(deeb)_3](ClO_4)_2$ begins to precipitate as the reaction proceeds toward completion, leaving behind unreacted ligand in solution and allowing for facile isolation of the metal complex. The compound is surprisingly soluble in CH_2Cl_2 , so oxidation of $[Co(deeb)_3]^{2+}$ was achieved by the addition of $NOPF_6$ to the solution. As oxidation proceeds, $[Co(deeb)_3]^{3+}$ precipitates from CH_2Cl_2 as a mixed ClO_4/PF_6 salt which can be fully converted to the desired PF_6^- salt using an aqueous saturated solution of KPF_6 .

The synthesis of [Co(pyrro-bpy)₃]²⁺ has been previously reported but we were unable to find any reference to the

Co(III) form. The Co(II) complex was originally synthesized using the pre-formed pyrro-bpy ligand and complexing to Co(II); however, we developed an alternate route for the formation of the Co(III) complex due to concerns about side reactions associated with the pyrrolidinyl nitrogen during oxidation from Co(II) to Co(III). We therefore prepared $[\text{Co}(4,4'-\text{Cl}_2\text{-bpy})_3]^{3+}$ as a starting point. The Co(III) center activates the 4 and 4' positions on the bpy backbone for substitution by the pyrrolidine as evidenced by the immediate color change from yellow to orange upon addition of the pyrrolidine to a methanolic solution of the $[\text{Co}(4,4'-\text{Cl}_2\text{-bpy})_3]^{3+}$. Due to the formation of HCl in the substitution reaction, a slight excess of pyrrolidine was used to ensure that

Table 1. Ligand-Field Transition Energies and Parameters for Co(lll) Complexes in CH₃CN Solution Calculated Using Diagonal Expressions^a

complex	${}^{3}T_{1}$	$^{3}T_{2}$	$^{1}T_{1}$	${}^{1}T_{2}$	10 Dq	В	eta^b	С	C/B
$[Co(acac)_3]^c$	9450	12 550	16 880	23 010	20 600	390	0.36	3720	9.6
$[Co(pyrro-bpy)_3](PF_6)_3$	13 010	16 240	20 100		23 650	400	0.37	3550	8.8
$[Co(NH_3)_6]Cl_3^d$	13 640	17 440	21 050	29 500	24 760	475	0.44	3710	7.8
$[Co(phen)_3](PF_6)_3$	13 950	17 070	21 430		25 170	390	0.36	3740	9.6
$[Co(dtb)_3](PF_6)_3$	14 540	17 080	21 650		25 200	320	0.29	3550	11.2
$[Co(en)_3]Cl_3^d$	13 920	17 300	21 460	29 590	25 230	420	0.39	3770	8.9
$[Co(5,5'-dmb)_3](PF_6)_3$	14 420	17 390	21 820		25 510	370	0.34	3700	9.9
$[Co(OMe-bpy)_3](PF_6)_3$	13 650	17 220	21 580		25 550	450	0.41	3970	8.9
$[Co(4,4'-dmb)_3](PF_6)_3$	14 600	17 750	21 960		25 640	390	0.36	3680	9.4
$[Co(bpy)_3](PF_6)_3$	13 770	17 490	21 860		25 900	470	0.43	4050	8.7
$[Co(deeb)_3](PF_6)_3$	14 910	18 220	22 170		25 800	410	0.38	3630	8.8
$[Co(terpy)_2](PF_6)_3$	15 560		23 000		26 750			3730	
$[Co(B^{Me}ImPy)_2](PF_6)_3$	19 940		26 830		30 270			3450	
$K_3[Co(CN)_6]^{d,e}$	25 470		31 830	39 240	35 010	460	0.43	3180	6.9

^aAII values reported in cm⁻¹. ^bCalculated using eq 6 with a value of B₀ = 1080 cm⁻¹. ^cSpectrum recorded in CHCl₃ solution. ^dSpectrum recorded in H₂O solution. eTransition energies taken from refs 53 and 54.

all of the pyrrolidinyl nitrogen atoms were deprotonated in the isolated complex.

The synthesis of [Co(BMeImPy)₂](PF₆)₃ started with deprotonation of the carbene ligand using LiHMDS at a low temperature. The addition of anhydrous CoBr2 initiated the formation of the desired Co(II) complex, which manifested as a dark green solution as the reaction mixture was slowly warmed to room temperature. Due to the strong σ -donation from the carbene, the complex was easily oxidized to Co(III) by simply bubbling air into the solution, whereupon the dark green solution slowly changed to a light brown and began to precipitate as the oxidation proceeded. The overall reaction was not as clean as for the other two compounds, as purification required two initial recrystallizations to remove a dark, slightly tacky material which then allowed for better separation on a Sephadex LH-20 size-exclusion column. Two bands—the first dark yellow in color and the second also yellow but less intense-moved closely together on the column. The first eluent contained the desired compound but also contained unidentified impurities, while the second contained a more highly purified form of the compound. Recrystallization of the material obtained from this second band afforded the analytically pure material for use in our

The structures of the cations of all three of these compounds are unremarkable, with metal-ligand bond distances and angles about the primary coordination sphere consistent with low-spin Co(III). Representations of the cations of [Co(pyrrobpy)₃](PF₆)₃ and $[Co(B^{Me}ImPy)_2](PF_6)_3$ are shown in Figure 4; additional details concerning refinement, metrics, and drawings of the cations for all three complexes can be found in the Supporting Information.

 π -Donors vs π -Acceptors and Their Net Influence in the First-Transition Series. The molecules contained in our series of 14 compounds were chosen to span a reasonably wide range of substituents from strongly π -donating in the case of 4,4'-dipyrrolidinyl-2,2'-bipyridine (pyrro-bpy) to π acids such as 4,4'-diethylester-2,2'-bipyridine (deeb), as well as ligands devoid of π interactions (e.g., NH₃ and ethylenediamine). Extremes in σ -donating and π -accepting character were also included in the cases of $[Co(B^{Me}ImPy)_2]^{3+}$ and $[Co(CN)_6]^{3-}$, respectively, as a means for comparison. We acquired

absorption spectra for the entire series and analyzed them following the same protocol outlined above for $[Co(bpy)_3]^{3+}$. The ligand-field parameters obtained from both diagonal and full-matrix analyses of the deconvolved spectra are collected in Tables 1 and 2, respectively; the experimental spectra and

Table 2. Ligand-Field Transition Energies and Parameters for Co(lll) Complexes in CH₃CN Solution Calculated from Full Diagonalization Analysis

complex	10 Dq	В	β	С	C/B	
[Co(acac) ₃]	19 210	480	0.44	3590	7.5	
$[Co(pyrro-bpy)_3](PF_6)_3$	22 440	480	0.45	3430	7.1	
$[Co(NH_3)_6]Cl_3$	23 430	580	0.53	3550	6.2	
$[Co(phen)_3](PF_6)_3$	23 940	460	0.43	3630	7.9	
$[Co(en)_3]Cl_3$	23 950	500	0.46	3640	7.3	
$[Co(dtb)_3](PF_6)_3$	24 130	370	0.34	3480	9.5	
$[Co(OMe-bpy)_3](PF_6)_3$	24 170	530	0.50	3830	7.2	
$[Co(5,5'-dmb)_3](PF_6)_3$	24 330	430	0.40	3600	8.3	
$[Co(4,4,-dmb)_3](PF_6)_3$	24 450	460	0.43	3570	7.8	
$[Co(bpy)_3](PF_6)_3$	24 480	560	0.52	3900	7.0	
$[Co(deeb)_3](PF_6)_3$	24 620	490	0.45	3520	7.2	
$K_3[Co(CN)_6]$	34 160	510	0.47	3080	6.1	
^a AII values reported in cm ⁻¹ .						

Tanabe-Sugano diagrams constructed for each compound based on these parameters can be found in the Supporting Information. In two of these cases— $[Co(terpy)_2]^{3+}$ and [Co(BMeImPy)₂]³⁺—the overlapping nature of the absorption features prevented us from assigning with confidence the minimum number of three ligand-field bands needed to specify values for 10 Dq and the Racah B and C parameters. Inspection of eqs 5 reveals that the ${}^{1}A_{1} \rightarrow {}^{3}T_{1}$ and ${}^{1}A_{1} \rightarrow {}^{1}T_{1}$ transitions do not depend on the Racah B parameter, so we were able to focus on these two transitions in $[Co(terpy)_2]^{3+}$ and $[Co(B^{Me}ImPy)_2]^{3+}$ to afford quantitative values for 10 Dq and Racah C for these compounds.

Inspection of the data in Tables 1 and 2 reveals a fairly narrow spread in the magnitude of ligand-field splitting (i.e., 10 Dq) despite the substantial change in the nature of the substituents on the aromatic ligands. Excluding the carbenebased B^{Me}ImPy complex and [Co(CN)₆]³⁻, there is only a

~3000 cm⁻¹ range covered by this series of low-spin complexes based on the diagonal terms (Table 1); this spread is attenuated to slightly more than 2000 cm⁻¹ for the full-matrix analysis (Table 2). This observation, coupled with the fact that compounds such as $[\text{Co(NH}_3)_6]^{3+}$ and $[\text{Co(en)}_3]^{3+}$ lie in the middle of the series in terms of the magnitude of 10 Dq, suggests that π bonding plays a relatively minor role (at least in terms of absolute contributions) in determining the ligand-field strength presented by polypyridyl ligands of this type to Co(III). Qualitatively this is to be expected given the more ionic nature of the bonding in complexes of the first-transition series compared to their second- and third-row congeners, but the overall lack of sensitivity of 10 Dq to the specific changes introduced into the ligand backbone across this series was unexpected.

More surprising than the limited range of ligand-field splitting was the apparent nature of the π interactions that are present. To understand the effect we believe is operative, one needs to consider several aspects of the electronic properties of the ligands that are relevant for determining d-orbital splitting in these compounds. As mentioned above, we interpret the range of 10 Dq accessible across the series of complexes we've prepared as an indication of a minor role for π bonding in an absolute sense. That stated, inspection of trends within the series of compounds does reveal an influence from π -based interactions in terms of their relative energetics. Consider first what would be expected in the absence of any π interactions. Although there are several factors that influence the magnitude of ligand-field splitting due to σ bonding, the d-orbital splitting should roughly correlate with the basicity of the donor atoms (i.e., the stronger the base, the larger the ligand-field splitting). The strength of pyridyl-based ligands acting as Lewis bases to a metal center can be gauged from their pK_h values (or, more conveniently, the pK_a values of the corresponding bipyridinium salts). Table 3 lists pK_a values of the hydrochloride salts of

Table 3. pK_a Values of Selected Polypyridyl Ligands^a

ligand	pK_a	$pK_a^L - pK_a^{bPy}$
phen	4.53	0.91
4,4'-dmb	4.40	0.78
5,5′-dmb	3.97	0.35
bрy	3.62	0
deeb	2.45	-1.17
^a From ref 55.		

several of the ligands used in our study. 55 Not surprisingly, the strongest acid is 4,4'-diethylester-2,2'-bipyridinium chloride, where the electron-withdrawing characteristics of the ester groups attenuate the donor ability of the nitrogen atoms by more than an order of magnitude relative to 2,2'-bipyridine. The introduction of CH₃ groups (i.e., 5,5'- and 4,4'-dimethyl) increases the ligand's basicity relative to the unsubstituted ligand, as might be expected given their electron-donating properties. At the other end of the spectrum is 1,10phenanthroline. While not a straightforward comparison due to structural differences compared to the bpy derivatives, it is nevertheless roughly 2 orders of magnitude more basic than deeb. If π interactions were irrelevant, the expectation would be that measured values of 10 Dq for Co(III) complexes composed of this subset of compounds should follow a qualitatively predictable trend from largest (phen) to smallest (deeb). Inspection of Tables 1 and 2 reveals that this is the

exact opposite trend of what is measured for 10 Dq across this series. While the correlation is not quantitatively robust, $[\text{Co}(\text{deeb})_3]^{3+}$ exhibits the largest value of 10 Dq for this series, while $[\text{Co}(\text{phen})_3]^{3+}$ exhibits the smallest. Again, the variations are not large, but π interactions between the ligand and metal are clearly sufficient to modulate the ligand-field splitting of these compounds in a manner that opposes the predicted trend based on σ interactions alone.

To identify the nature of the π effect, we first consider the compound with the smallest ligand-field splitting, [Co(pyrrobpy)₃]³⁺. The lone pair associated with the ternary nitrogen of the pyrrolidine ring coupled with its location at the 4 and 4' positions of bipyridine makes this substituent an effective π donor to the ligand, which means that pyrro-bpy is expected to be more electron-rich than the unsubstituted form of the ligand as a result. The question is whether this makes pyrrobpy a stronger π -donor to Co(III) or a weaker π -acceptor. The same argument applies to [Co(deeb)₃]³⁺, i.e., is the more electron-deficient nature of deeb make it a better π -acceptor or a weaker π -donor? Either of these scenarios would result in shifts of the t_{2g} orbitals of the metal center in the appropriate direction to rationalize the changes in 10 Dq that are experimentally observed. This question is difficult to answer in isolation—something akin to asking if an answer of 4 is achieved from the sum of 3 and 1 or 6 and -2—but is important from the point of view of ligand design. Should we view polypyridyl ligands bound to first-row metals as net π donors or net π -acceptors in terms of their influence on the electronic structure of the resulting metal complex?

We believe the answer to this question can be found in the data presented in Table 1, specifically in the parameters derived for $[Co(terpy)_2]^{3+}$. To understand this, consider first the electronic structure of [Ru(terpy)₂]²⁺. This compound, which has been well studied by many groups in a variety of contexts over the years, 56-60 represents an outlier when it comes to the photophysics of Ru(II) polypyridyls in terms of the surprisingly short lifetime of its lowest-lying ³MLCT excited state. In contrast to [Ru(bpy)₃]²⁺, whose ³MLCT state persists for ~ 1 μ s in deoxygenated solution at room temperature, the corresponding lifetime for [Ru(terpy)₂]²⁺ is ~250 ps. 61 This dramatically reduced lifetime relative to [Ru(bpy)₃]²⁺ has been attributed to thermal accessibility of the lowest-energy ³T₁ ligand-field state from the charge-transfer manifold, resulting in a significantly larger value for the rate constant for nonradiative decay $(k_{\rm nr})$ for the ${}^3{\rm MLCT}$ state. 62,63 Apart from the consequences of this as it pertains to the excited-state properties of [Ru(terpy)₂]²⁺ (e.g., significantly attenuated emission, limited utility for biomolecular photoredox chemistry, etc.), the difference in photophysical behavior indicates that terpy presents a much weaker ligand field to Ru(II) than bpy. The reason for this is believed to be associated with the structural constraints endemic to the terpy ligand as evidenced by restricted N-Ru-N bond angles of ca. 80 and 160° for cis and trans, respectively, resulting in relatively poor metal-ligand overlap affecting both σ -donation from the nitrogen atoms and π -backbonding from the metal into the π^* orbital(s) of the ligand.⁶⁴

In contrast, the data we have acquired on $[Co(bpy)_3]^{3+}$ and $[Co(terpy)_2]^{3+}$ exhibits the exact opposite relationship from what is inferred for their Ru(II) analogs. While the absorption spectrum of $[Co(terpy)_2]^{3+}$ does not allow for detection of the three transitions needed to independently assess the Racah B and C parameters, we were able to quantify that the broadest

Table 4. Comparison of Structural Parameters for [Ru(terpy)₂]²⁺ and [Co(terpy)₂]³⁺

	average					
complex	M-N _{axial} (Å)	$M-N_{eq}$ (Å)	N_{axial} -M- N_{axial} (deg)	N_{eq} -M- N_{eq} (deg)	N _{eq} -M-N _{axial} (deg)	
$[Ru(terpy)_2]^{2+a}$	1.968	2.074	178.04	157.77	78.9	
$[Co(terpy)_2]^{3+b}$	1.856	1.943	178.41	165.55	82.8	
difference (Ru-Co)	0.112	0.131	-0.37	-7.78	-3.9	
^a From ref 65. ^b From ref 3	3.					

measure of ligand-field strength—10 Dq—is ~1000 cm⁻¹ larger for $[Co(terpy)_2]^{3+}$ than $[Co(bpy)_3]^{3+}$. The steric constraints associated with terpy binding to Co(III) are very similar to that for Ru(II) (Table 4), so the same attenuation in metal—ligand interactions due to distortions from octahedral geometry identified for $[Ru(terpy)_2]^{2+}$ should be operative for $[Co(terpy)_2]^{3+}$. But, rather than leading to a reduction in ligand-field strength relative to bpy as is seen for Ru(II), the net result in the case of Co(III) is an increase in that same parameter. These observations lead us to the conclusion that terpy must act as a net π -donor to Co(III): only in this circumstance can one easily rationalize how an attenuation in a metal—ligand interaction can lead to a larger ligand-field strength.

Indeed, we believe that net donation is the primary mode of π interactions between Co(III) and all of the polypyridyl-based ligands being considered herein; the variation in 10 Dq across the different substituents noted above is therefore not associated with changes in the π -accepting nature of the ligand but rather due to modulations in their ability to act as a π base. The likely origin of this effect—and by extension the reason for the reversal in behavior between metal polypyridyl complexes of the first- and second-transition series—is the shift in the energy of the t_{2g} -symmetry d orbitals as a function of charge and principal quantum number. Both the filled π and unfilled π^* orbitals of the polypyridyl ligands are of the appropriate symmetry to interact with, in the case of a low-spin d^6 ion, the filled t_{2g} orbitals of the metal center. Whether a ligand like 2,2'-bipyridine acts as a net π -donor or π -acceptor in a given compound will therefore reflect a balance of interactions that will depend on the energy of the metal-based t_{2g} orbitals relative to these ligand-based π and π^* orbitals. For the two metal ions being compared here, the higher valence orbital ionization energy of Co(III) compared to Ru(II) indicates that the d-orbitals of Co(III) are significantly lower in energy, 67,68 which we believe results in a more favorable energetic match with the filled π orbitals of the polypyridyl ligands and trends in 10 Dq that are consistent with net π donation. This picture inverts for Ru(II) due to the increase in principal quantum number coupled with the decrease in ionic charge, thereby raising the energy of the d orbitals to where the $d-\pi^*$ gap defines the dominant interaction. It should be noted that the idea of considering polypyridyl ligands like bpy as net π -donors to first-row metals was previously suggested by Jakubikova and co-workers based on their computational studies of Fe(II) complexes.⁶⁶ Although our measurements were carried out on Co(III) complexes, we nevertheless view our results as experimental support for their conclusions.

Trends in the Racah B and C Parameters... or Not. The most challenging aspect associated with analyzing the data on the series of compounds we have prepared and characterized is the significance (if any) of variations in the Racah B and C parameters listed in Tables 1 and 2. As mentioned previously, these two parameters correspond to the linear combinations of

electron—electron repulsion integrals indicated in eqs 3. These parameters were originally defined in this manner primarily to simplify spectral analyses in the weak-field limit, but researchers have since tried to ascribe a deeper physical significance to the numerical values obtained. These efforts have largely focused on the B parameter, in large part because reliable data on the C parameter is relatively scarce. The B values of a given transition-metal complex are typically compared to the corresponding values for the free ion, B_0 , in the form of a ratio defined as

$$\beta = \frac{B}{B_0} \tag{6}$$

The B value for a compound is almost invariably smaller than B_0 ; since B is defined in terms of electron-electron repulsion integrals, the value of β has served as a qualitative assessment of the degree of covalency in the metal-ligand bonding interaction (the idea being increased covalency leads to greater delocalization of the d orbitals and therefore a reduction in the magnitude of electron-electron repulsion within the d-orbital manifold). Inspection of Tables 1 and 2 reveal that the experimental values for B for all of the compounds studied are significantly attenuated compared to the free-ion value of 1080 cm⁻¹ for Co(III), but there is no obvious correlation across the series with the notable exception that the two compounds devoid of π interactions—[Co- $(NH_3)_6]^{3+}$ and $[Co(en)_3]^{3+}$ —do exhibit larger values of B relative to most other members of the series. One could therefore speculate that this supports at least qualitatively the notion of B reflecting the extent of d-orbital interaction with the ligands, with the two σ -only complexes being the most ionic. That stated, we believe that a more detailed analysis of these data (including the physical significance of variations in the C parameter) would require an extensive theoretical effort that is well beyond the scope of the present study.

Insights into Ligand-Field Strengths for Iron(II). The broader goal of this study was to develop the means to assess ligand-field strengths in cases for which the requisite transitions are obscured by more intense absorption features (e.g., Fe(II) charge-transfer complexes). One way to achieve this is to find a few Fe(II) complexes wherein at least one ligand-field transition could be observed, then set up a correlation between the optical properties of the corresponding Co(III) complex. Although this approach would not be expected to be robust, it could still offer an approximation for the ligand-field strength of the Fe(II) complex where none would otherwise be available. We acquired an electronic absorption spectrum of [Fe(bpy)₃]²⁺ using the same approach as was done for the Co(III) complexes and were able to identify a reasonably welldefined feature centered at ~830 nm which we assign as the ${}^{1}A_{1} \rightarrow {}^{3}T_{1}$ absorption (Figure 5). This is consistent with the assignment of Palmer and Piper in their analysis of the singlecrystal absorption spectrum of [Fe(bpy)3]Cl2.69 The corre-

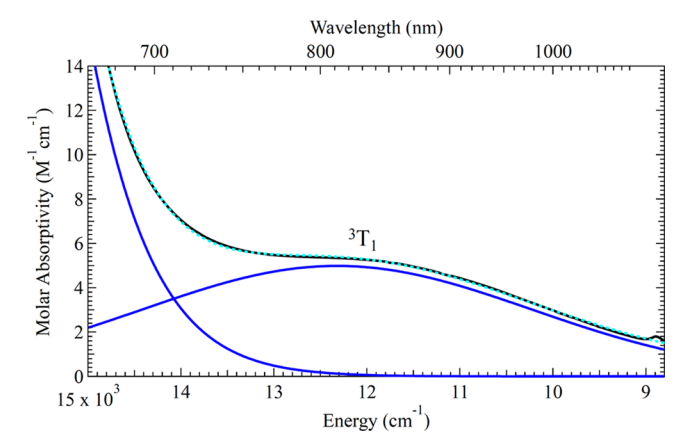


Figure 5. Near-IR electronic absorption spectrum of $[Fe(bpy)_3]^{2+}$ in CH₃CN solution obtained in a 10 cm pathlength cell at high concentration. The low extinction coefficient for the band centered at 830 nm is consistent with a spin-forbidden transition and is assigned as the ${}^{1}A_{1} \rightarrow {}^{3}T_{1}$ absorption.

sponding transition for [Co(bpy)₃]³⁺ sits at 730 nm, a value that allows us to infer a substantial decrease in 10 Dq upon replacement of Co(III) for Fe(II). With only one ligand-field band observed for [Fe(bpy)₃]²⁺, one cannot quantify its ligandfield parameters in the same way we were able to for [Co(bpy)₃]³⁺; however, we can approximate the positions of the 3T_2 and 1T_1 absorptions of [Fe(bpy)₃]²⁺ based on their observed locations in [Co(bpy)₃]³⁺. The expressions in eqs 5b-5d specify the energies for ground-state absorption to the ¹T₁, ³T₂, and ³T₁ states, respectively, of a d⁶ ion. If we take the ratio of the ${}^{3}T_{2}$ and ${}^{3}T_{1}$ transition energies of $[Co(bpy)_{3}]^{3+}$ (i.e., $E(^3T_2)/E(^3T_1)$) as well as that of the 1T_1 and 3T_1 states $(E(^{1}T_{1})/E(^{3}T_{1}))$, average them, then reference them to the observed ${}^{1}A_{1} \rightarrow {}^{3}T_{1}$ absorption of $[Fe(bpy)_{3}]^{2+}$, we can obtain approximate locations of the ${}^{1}A_{1} \rightarrow {}^{3}T_{2}$ and ${}^{1}A_{1} \rightarrow {}^{1}T_{1}$ absorptions for [Fe(bpy)₃]²⁺ and use those values to estimate a value of 10 Dq for $[\hat{F}e(\hat{b}py)_3]^{2+}$ of ~21 000 cm⁻¹. ⁷⁰ The data therefore indicate that replacing Co(III) with Fe(II) in the same ligand-field environment leads to a reduction in the magnitude of 10 Dq on the order of ~ 3000 cm⁻¹. While we concede that a comparison between two compounds does not provide the basis for any broad generalizations, we believe that information on the absorptive properties of a ligand system of interest bound to Co(III) nevertheless allows one to make a reasonable approximation of the ligand-field strength of the corresponding Fe(II) complex that would otherwise be exceedingly difficult to obtain.

Given the limited amount of information that exists for Fe(II) analogs, it is difficult to experimentally address the question of whether polypyridyl ligands behave as net π -donors or net π -acceptors when bound to Fe(II) as we did with Co(III). That stated, following the reasoning discussed above, the energies of the d orbitals of Fe(II) would be expected to lie between those of Co(III) and Ru(II), suggesting that these competing effects are likely close to offsetting each other in Fe(II). This circumstance would be consistent with results we have previously reported on ground-state recovery dynamics following photoexcitation of $[Fe(bpy)_3]^{2+}$ and $[Fe(4,4'-dmb)_3]^{2+}$, where a modest ~ 35 cm⁻¹ increase in the barrier associated with ground-state recovery for the latter suggested only a slightly weaker ligand field associated with 4,4'-dmb compared to bpy.

CONCLUSIONS

The synthesis and electronic absorption spectroscopy of a series of Co(III) complexes have been carried out in an effort to assess the field strength presented by ligands that are commonly used to create strong charge-transfer-based absorption cross sections in transition-metal complexes. The intensity of these bands coupled with their spectral location typically renders the observation of the ligand-field transitions necessary to make such an assessment difficult if not impossible for most chromophores of the first-transition series. This is particularly true in the case of the d⁶ configuration, complexes whose photophysical properties are of considerable interest for applications involving photoinduced electron transfer chemistry. The significant blueshift in the LMCT transition(s) of Co(III) complexes provided the mechanism by which the underlying ligand-field transitions could be observed and quantified. A detailed analysis of both spin-allowed and spin-forbidden d-d absorptions allowed for a quantitative measure of the ligand-field splitting parameter—10 Dq—as well as the Racah B and C terms that together provide a complete description of the energies of the multielectronic states that comprise the excited-state electronic manifolds of the compounds. It was found that the ligand-field strength imposed on Co(III) by polypyridyl ligands is ca. 25 000 cm⁻¹, a value that can be tuned by $\pm \sim 1500$ cm⁻¹ via substituent changes on the periphery of the aromatic residues. An unexpected outcome of this analysis was the observation that, while dominated by σ -based interactions between the lone pairs on the ligating nitrogen atoms and the metal center, ligands of this class behave as net π -donors to the metal. This stands in contrast to their net π -accepting character when bound to ions from the second- and third-transition series and represents an important conceptual shift for how to think about metal-ligand interactions for the purposes of ligand design. Results obtained on a carbene-based complex further establish experimentally the ability of these strong, σ -donating ligands to destabilize ligand-field excited states, thereby enhancing the utility of charge-transfer states for photochemical transformations. We believe that this approach of using Co(III) as a surrogate for ions such as Fe(II) will prove to be a useful tool for those seeking to manipulate the relative energetics of ligand-field and charge-transfer excited states to modulate photoredox activity of these earth-abundant compounds through targeted synthetic design.

ASSOCIATED CONTENT

Supporting Information

The Supporting Information is available free of charge at https://pubs.acs.org/doi/10.1021/jacs.2c04945.

X-ray crystallography; UV-vis spectra of studied complexes; Tanabe-Sugano diagrams; and ¹H NMR spectra of complexes (PDF)

Accession Codes

CCDC 2157807, 2158019, and 2161073 contain the supplementary crystallographic data for this paper. These data can be obtained free of charge via www.ccdc.cam.ac.uk/ data_request/cif, or by emailing data_request@ccdc.cam.ac. uk, or by contacting The Cambridge Crystallographic Data Centre, 12 Union Road, Cambridge CB2 1EZ, UK; fax: +44 1223 336033.

AUTHOR INFORMATION

Corresponding Author

James K. McCusker – Department of Chemistry, Michigan State University, East Lansing, Michigan 48824, United States; o orcid.org/0000-0002-5684-3117; Email: jkm@ chemistry.msu.edu

Author

Jonathan T. Yarranton – Department of Chemistry, Michigan State University, East Lansing, Michigan 48824, United States; orcid.org/0000-0003-3134-962X

Complete contact information is available at: https://pubs.acs.org/10.1021/jacs.2c04945

Notes

The authors declare no competing financial interest.

ACKNOWLEDGMENTS

The authors thank Professor Rémi Beaulac for many useful and stimulating discussions, particularly with regard to the implementation of the ligand-field analyses. They also thank Dr. Richard J. Staples of the Department of Chemistry's Center for Crystallographic Research for his assistance in the refinement of the reported structures. This research was generously supported by the Chemical Sciences, Geosciences, and Biosciences Division, Office of Basic Energy Science, Office of Science, U.S. Department of Energy under Grant No. DE-FG02-01ER15282. The Rigaku Synergy S Diffractometer was purchased with Support from the MRI program by the National Science Foundation under Grant No. CHE-1919565 for use at the Center for Crystallographic Research, MSU.

REFERENCES

- (1) Wenger, O. S. Is Iron the New Ruthenium? Chem. Eur. J. **2019**, 25, 6043-6052.
- (2) Wegeberg, C.; Wenger, O. S. Luminescent First-Row Transition Metal Complexes. JACS Au 2021, 1, 1860-1876.
- (3) Glaser, F.; Kerzig, C.; Wenger, O. S. Multi-Photon Excitation in Photoredox Catalysis: Concepts, Applications, Methods. Angew. Chem., Int. Ed. 2020, 59, 10266-10284.
- (4) Nazeeruddin, M. K.; Zakeeruddin, S. M.; Humphry-Baker, R.; Jirousek, M.; Liska, P.; Vlachopoulos, N.; Shklover, V.; Fischer, C.-H.; Grätzel, M. Acid-Base Equilibria of (2,2'-Bipyridyl-4,4'-Dicarboxylic Acid)Ruthenium(II) Complexes and the Effect of Protonation on Charge-Transfer Sensitization of Nanocrystalline Titania. Inorg. Chem. **1999**, 38, 6298-6305.
- (5) Kreitner, C.; Mengel, A. K. C.; Lee, T. K.; Cho, W.; Char, K.; Kang, Y. S.; Heinze, K. Strongly Coupled Cyclometalated Ruthenium Triarylamine Chromophores as Sensitizers for DSSCs. Chem. – Eur. J. **2016**, 22, 8915-8928.
- (6) Chan, A. Y.; Perry, I. B.; Bissonnette, N. B.; Buksh, B. F.; Edwards, G. A.; Frye, L. I.; Garry, O. L.; Lavagnino, M. N.; Li, B. X.; Liang, Y.; Mao, E.; Millet, A.; Oakley, J. V.; Reed, N. L.; Sakai, H. A.; Seath, C. P.; MacMillan, D. W. C. Metallaphotoredox: The Merger of Photoredox and Transition Metal Catalysis. Chem. Rev. 2022, 122, 1485-1542
- (7) Woodhouse, M. D.; McCusker, J. K. Mechanistic Origin of Photoredox Catalysis Involving Iron(II) Polypyridyl Chromophores. J. Am. Chem. Soc. 2020, 142, 16229-16233.
- (8) Gualandi, A.; Marchini, M.; Mengozzi, L.; Natali, M.; Lucarini, M.; Ceroni, P.; Cozzi, P. G. Organocatalytic Enantioselective Alkylation of Aldehydes with [Fe(bpy)3]Br2 Catalyst and Visible Light. ACS Catal. 2015, 5, 5927-5931.
- (9) Parisien-Collette, S.; Hernandez-Perez, A. C.; Collins, S. K. Photochemical Synthesis of Carbazoles Using an [Fe(phen)₃]-

- (NTf₂)₂/O₂ Catalyst System: Catalysis toward Sustainability. Org. Lett. 2016, 18, 4994-4997.
- (10) McCusker, J. K. Electronic Structure in the Transition Metal Block and Its Implications for Light Harvesting. Science 2019, 363,
- (11) Liu, Y.; Harlang, T.; Canton, S. E.; Chábera, P.; Suárez-Alcántara, K.; Fleckhaus, A.; Vithanage, D. A.; Göransson, E.; Corani, A.; Lomoth, R.; Sundström, V.; Wärnmark, K. Towards Longer-Lived Metal-to-Ligand Charge Transfer States of Iron(II) Complexes: An N-Heterocyclic Carbene Approach. Chem. Commun. 2013, 49, 6412-
- (12) Herr, P.; Glaser, F.; Büldt, L. A.; Larsen, C. B.; Wenger, O. S. Long-Lived, Strongly Emissive, and Highly Reducing Excited States in Mo(0) Complexes with Chelating Isocyanides. J. Am. Chem. Soc. 2019, 141, 14394-14402.
- (13) Reuter, T.; Kruse, A.; Schoch, R.; Lochbrunner, S.; Bauer, M.; Heinze, K. Higher MLCT Lifetime of Carbene Iron(II) Complexes by Chelate Ring Expansion. Chem. Commun. 2021, 57, 7541-7544.
- (14) Steube, J.; Burkhardt, L.; Päpcke, A.; Moll, J.; Zimmer, P.; Schoch, R.; Wölper, C.; Heinze, K.; Lochbrunner, S.; Bauer, M. Excited-State Kinetics of an Air-Stable Cyclometalated Iron(II) Complex. Chem. - Eur. J. 2019, 25, 11826-11830.
- (15) Vukadinovic, Y.; Burkhardt, L.; Päpcke, A.; Miletic, A.; Fritsch, L.; Altenburger, B.; Schoch, R.; Neuba, A.; Lochbrunner, S.; Bauer, M. When Donors Turn into Acceptors: Ground and Excited State Properties of Fe^{II} Complexes with $\bar{\text{A}}$ Amine-Substituted Tridentate Bis-Imidazole-2-Ylidene Pyridine Ligands. Inorg. Chem. 2020, 59, 8762-
- (16) Braun, J. D.; Lozada, I. B.; Herbert, D. E. In Pursuit of Panchromatic Absorption in Metal Coordination Complexes: Experimental Delineation of the HOMO Inversion Model Using Pseudo-Octahedral Complexes of Diarylamido Ligands. Inorg. Chem. 2020, 59, 17746-17757.
- (17) Braun, J. D.; Lozada, I. B.; Kolodziej, C.; Burda, C.; Newman, K. M. E.; van Lierop, J.; Davis, R. L.; Herbert, D. E. Iron(II) Coordination Complexes with Panchromatic Absorption and Nanosecond Charge-Transfer Excited State Lifetimes. Nat. Chem. 2019, 11, 1144-1150.
- (18) Magra, K.; Francés-Monerris, A.; Cebrián, C.; Monari, A.; Haacke, S.; Gros, P. C. Bidentate Pyridyl-NHC Ligands: Synthesis, Ground and Excited State Properties of Their Iron(II) Complexes and the Role of the Fac/Mer Isomerism. Eur. J. Inorg. Chem. 2022, 2022, No. e202100818.
- (19) Liu, L.; Duchanois, T.; Etienne, T.; Monari, A.; Beley, M.; Assfeld, X.; Haacke, S.; Gros, P. C. A New Record Excited State ³MLCT Lifetime for Metalorganic Iron(II) Complexes. Phys. Chem. Chem. Phys. 2016, 18, 12550-12556.
- (20) Paulus, B. C.; Adelman, S. L.; Jamula, L. L.; McCusker, J. K. Leveraging Excited-State Coherence for Synthetic Control of Ultrafast Dynamics. Nature 2020, 582, 214-218.
- (21) Paulus, B. C.; Nielsen, K. C.; Tichnell, C. R.; Carey, M. C.; McCusker, J. K. A Modular Approach to Light Capture and Synthetic Tuning of the Excited-State Properties of Fe(II)-Based Chromophores. J. Am. Chem. Soc. 2021, 143, 8086-8098.
- (22) Hauser, A. Reversibility of Light-Induced Excited Spin State Trapping in the $Fe(Ptz)_6(BF_4)_2$, and the $Zn_{1-x}Fe_x(Ptz)_6(BF_4)_2$ Spin-Crossover Systems. Chem. Phys. Lett. 1986, 124, 543-548.
- (23) Hauser, A. Intersystem Crossing in the [Fe(Ptz)₆](BF₄)₂ Spin Crossover System (Ptz=1-propyltetrazole). J. Chem. Phys. 1991, 94, 2741-2748.
- (24) Klaeui, W.; Eberspach, W.; Guetlich, P. Spin-Crossover Cobalt(III) Complexes: Steric and Electronic Control of Spin State. Inorg. Chem. 1987, 26, 3977-3982.
- (25) Oki, A. R.; Morgan, R. J. An Efficient Preparation of 4,4'-Dicarboxy-2,2'-Bipyridine. Synth. Commun. 1995, 25, 4093-4097.
- (26) Worl, L. A.; Duesing, R.; Chen, P.; Ciana, L.; Meyer, T. J. Photophysical Properties of Polypyridyl Carbonyl Complexes of Rhenium(I). J. Chem. Soc., Dalton Trans. 1991, 849-858.

- (27) Zhang, D.; Dufek, E. J.; Clennan, E. L. Syntheses, Characterizations, and Properties of Electronically Perturbed 1,1'-Dimethyl-2,2'-bipyridinium Tetrafluoroborates. J. Org. Chem. 2006, 71, 315-319.
- (28) Peris, E.; Mata, J.; Loch, J. A.; Crabtree, R. H. A Pd Complex of a Tridentate Pincer CNC Bis-Carbene Ligand as a Robust Homogenous Heck Catalyst. Chem. Commun. 2001, 201-202.
- (29) Bjerrum, J.; McReynolds, J. P.; Oppegard, A. L.; Parry, R. W.Hexamminecobalt(III) Salts. In Inorganic Syntheses, Wiley, 1946; Vol. 2, pp 216-221.
- (30) Work, J. B.; McReynolds, J. P. Tris(Ethylenediamine)Cobalt-(III) Chloride. In Inorganic Syntheses, Wiley, 1946; Vol. 2, pp 221-
- (31) Bella, F.; Vlachopoulos, N.; Nonomura, K.; Zakeeruddin, S. M.; Grätzel, M.; Gerbaldi, C.; Hagfeldt, A. Direct Light-Induced Polymerization of Cobalt-Based Redox Shuttles: An Ultrafast Way towards Stable Dye-Sensitized Solar Cells. Chem. Commun. 2015, 51, 16308-16311.
- (32) Panja, A. Mononuclear Cobalt(III) and Iron(II) Complexes with Diimine Ligands: Synthesis, Structure, DNA Binding and Cleavage Activities, and Oxidation of 2-Aminophenol. Polyhedron **2012**, 43, 22-30.
- (33) Constable, E. C.; Harris, K.; Housecroft, C. E.; Neuburger, M.; Zampese, J. A. Turning $\{M(Tpy)_2\}^{n+}$ Embraces and $CH \cdots \pi$ Interactions on and off in Homoleptic Cobalt(II) and Cobalt(III) Bis(2,2':6',2"-Terpyridine) Complexes. CrystEngComm 2010, 12, 2949-2961.
- (34) Burschka, J.; Kessler, F.; Baranoff, E.; Nazeeruddin, M. K.; Graetzel, M. Metal Complexes for Use as Dopants and Other Uses. WIPO Patent WO2012/114316 A1, 2012.
- (35) Wong, K. W.; Wong, M. C. Cobalt-Polypyridyl Complex for Treatment of Cancer, A Pharmaceutical Composition and a Kit Comprising It. U.S. Patent US2018/0050044 A1, 2018.
- (36) Sheldrick, G. M. SHELXT Integrated Space-Group and Crystal-Structure Determination. Acta Crystallogr., Sect. A 2015, A71,
- (37) Dolomanov, O. V.; Bourhis, L. J.; Gildea, R. J.; Howard, J. A. K.; Puschmann, H. OLEX2: A Complete Structure Solution, Refinement and Analysis Program. J. Appl. Crystallogr. 2009, 42,
- (38) Sheldrick, G. M. Crystal Structure Refinement with SHELXL. Acta Crystallogr., Sect. C 2015, C71, 3-8.
- (39) COSMO V1.61, Software for the CCD Detector Systems for Determining Data Collection Parameters; Bruker Analytical X-ray Systems: Madison, WI, 2009.
- (40) APEX2 V2010.11-3, Software for the CCD Detector System; Bruker Analytical X-ray Systems: Madison, WI, 2010.
- (41) SAINT V7.68A, Software for the Integration of CCD Detector System; Bruker Analytical X-ray Systems: Madison, WI, 2010.
- (42) Blessing, R. H. An Empirical Correction for Absorption Anisotropy. Acta Crystallogr., Sect. A 1995, 51, 33-38.
- (43) Bethe, H. Termaufspaltung in Kristallen. Ann. Phys. 1929, 395, 133 - 208.
- (44) Condon, E. U.; Shortley, G. H. The Theory of Complex Spectra II. Phys. Rev. 1931, 37, 1025-1043.
- (45) Racah, G. Theory of Complex Spectra. II. Phys. Rev. 1942, 62,
- (46) Jørgensen, C. K.; Wickberg, B.; et al. Studies of Absorption Spectra VIII. Three and More d-Electrons in Cubic Crystal Fields. Acta Chem. Scand. 1955, 9, 116-121.
- (47) Ballhausen, C. J. Introduction to Ligand Field Theory, McGraw-Hill Book Company, Inc., 1962.
- (48) Griffith, J. S.; Orgel, L. E. Ligand-Field Theory. Q. Rev. Chem. Soc. 1957, 11, 381-393.
- (49) Tanabe, Y.; Sugano, S. On the Absorption Spectra of Complex Ions. I. J. Phys. Soc. Jpn. 1954, 9, 753-766.
- (50) Tanabe, Y.; Sugano, S. On the Absorption Spectra of Complex Ions II. J. Phys. Soc. Jpn. 1954, 9, 766-779.

- (51) Schmidtke, H.-H. The Variation of Slater-Condon Parameters F^k and Racah Parameters B and C with Chemical Bonding in Transition Group Complexes Mingos, D. M. P.; Schönherr, T., Eds.; Springer: Berlin, 2004.
- (52) Bendix, J. LIGFIELD, version 092; Copenhagen, Denmark, 1993.
- (53) Alexander, J. J.; Gray, H. B. Electronic Structures of Hexacyanometalate Complexes. J. Am. Chem. Soc. 1968, 90, 4260-
- (54) Miskowski, V. M.; Gray, H. B.; Wilson, R. B.; Solomon, E. I. Position of the ${}^{3}T_{1g} \leftarrow {}^{1}A_{1g}$ Transition in Hexacyanocobaltate(III). Analysis of Absorption and Emission Results. Inorg. Chem. 1979, 18, 1410-1412.
- (55) James, B. R.; Williams, R. J. P. 383. The Oxidation-Reduction Potentials of Some Copper Complexes. J. Chem. Soc. 1961, 0, 2007-
- (56) Stone, M. L.; Crosby, G. A. Charge-Transfer Luminescence from Ruthenium(II) Complexes Containing Tridentate Ligands. Chem. Phys. Lett. 1981, 79, 169-173.
- (57) Young, R. C.; Nagle, J. K.; Meyer, T. J.; Whitten, D. G. Electron Transfer Quenching of Nonemitting Excited States of Ru(TPP)(py)2 and Ru(trpy)₂²⁺. J. Am. Chem. Soc. 1978, 100, 4773-4778.
- (58) Kirchhoff, J. R.; McMillin, D. R.; Marnot, P. A.; Sauvage, J.-P. Photochemistry and Photophysics of Bis(Terpyridyl) Complexes of Ru(II) in Fluid Solution. Evidence for the Formation of an η^2 -Diphenylterpyridine Complex. J. Am. Chem. Soc. 1985, 107, 1138-
- (59) Vallett, P. J.; Damrauer, N. H. Experimental and Computational Exploration of Ground and Excited State Properties of Highly Strained Ruthenium Terpyridine Complexes. J. Phys. Chem. A 2013, 117, 6489-6507.
- (60) Lin, C.-T.; Böttcher, W.; Chou, M.; Creutz, C.; Sutin, N. Mechanism of the Quenching of the Emission of Substituted Polypyridineruthenium(II) Complexes by Iron(III), Chromium(III), and Europium(III) Ions. J. Am. Chem. Soc. 1976, 98, 6536-6544.
- (61) Winkler, J. R.; Netzel, T. L.; Creutz, C.; Sutin, N. Direct Observation of Metal-to-Ligand Charge-Transfer (MLCT) Excited States of Pentaammineruthenium(II) Complexes. J. Am. Chem. Soc. 1987, 109, 2381-2392.
- (62) Hewitt, J. T.; Vallett, P. J.; Damrauer, N. H. Dynamics of the ³MLCT in Ru(II) Terpyridyl Complexes Probed by Ultrafast Spectroscopy: Evidence of Excited-State Equilibration and Interligand Electron Transfer. J. Phys. Chem. A 2012, 116, 11536-11547.
- (63) Amini, A.; Harriman, A.; Mayeux, A. The Triplet Excited State of Ruthenium(II) Bis(2,2':6',2"-Terpyridine): Comparison between Experiment and Theory. Phys. Chem. Chem. Phys. 2004, 6, 1157-1164.
- (64) Islam, A.; Ikeda, N.; Yoshimura, A.; Ohno, T. Nonradiative Transition of Phosphorescent Charge-Transfer States of Ruthenium-(II)-to-2,2'-Biquinoline and Ruthenium(II)-to-2,2':6',2"-Terpyridine in the Solid State. Inorg. Chem. 1998, 37, 3093-3098.
- (65) Alatrash, N.; Macdonnell, F. M.CCDC 765853: CSD Communication, 2021. DOI: 10.5517/ccdc.csd.cc28mrk7.
- (66) Ashley, D. C.; Jakubikova, E. Tuning the Redox Potentials and Ligand Field Strength of Fe(II) Polypyridines: The Dual π -Donor and π-Acceptor Character of Bipyridine. Inorg. Chem. 2018, 57, 9907-9917.
- (67) Klasinc, L.; Novak, I.; Rieger, J.; Scholz, M. MO-Berechnungen an Heterocyclen, 24. Mitt.: Eine Interpretation der UPS Der 2,2'-Und 4,4'-Bipyridyle dnd deren N-Monoxide. Monatsh. Chem. 1981, 112, 697-705.
- (68) Gray, H. B. Electrons and Chemical Bonding Stevens, L., Ed.; W. A. Benjamin Inc.: New York, 1965.
- (69) Palmer, R. A.; Piper, T. S. 2,2'-Bipyridine Complexes. I. Polarized Crystal Spectra of Tris (2,2'-Bipyridine)Copper(II), -Nickel(II), -Cobalt(II), -Iron(II), and -Ruthenium(II). Inorg. Chem. **1966**, 5, 864-878.

(70) Using the average energy ratios of the Co(III) series, i.e., $E(^3T_2)/E(^3T_1)=1.24$ and $E(^1T_1)/E(^3T_1)=1.53$, the 3T_2 transition is calculated at 15 310 cm $^{-1}$ and the 1T_1 is calculated at 18 890 cm $^{-1}$. (71) Carey, M. C.; Adelman, S. L.; McCusker, J. K. Insights into the Excited-state Dynamics of Fe(II) Polypyridyl Complexes from Variable-tempertaure Ultrafast Spectroscopy. *Chem. Sci.* **2019**, *10*, 134–144.

□ Recommended by ACS

A Theoretical Assessment of Spin and Charge States in Binuclear Cobalt–Ruthenium Complexes: Implications for a Creutz–Taube Model Ion Separated by a $\rm C_{60}$ -De...

Alexsandro R. da Silva, Roberto Rivelino, et al.

DECEMBER 09, 2020

THE JOURNAL OF PHYSICAL CHEMISTRY A

Excitation-Wavelength-Dependent Photophysics of d^8d^8 Di-isocyanide Complexes

Martin Pižl, Antonín Vlček, et al.

DECEMBER 14, 2021

INORGANIC CHEMISTRY

READ 🗹

Spectroscopic Signatures of Resonance Inhibition Reveal Differences in Donor-Bridge and Bridge-Acceptor Couplings

David A. Shultz, Roger D. Sommer, et al.

FEBRUARY 18, 2020

JOURNAL OF THE AMERICAN CHEMICAL SOCIETY

READ 🗹

Solvent-Induced Redox Isomerism of Cobalt Complexes with Redox-Active Bisguanidine Ligands

Lukas Lohmeyer, Hans-Jörg Himmel, et al.

MAY 25, 2022

INORGANIC CHEMISTRY

READ 🗹

Get More Suggestions >